Lečić, M. R., *et al.*: An Experimental Investigation and Statistical Analysis…
THERMAL SCIENCE, Year 2017, Vol. 21, Suppl. 3, pp. S691-S704

S691

# AN EXPERIMENTAL INVESTIGATION AND STATISTICAL ANALYSIS OF TURBULENT SWIRL FLOW IN A STRAIGHT PIPE

by

## *Milan R. LEČIĆ* \*, *Aleksandar S. ĆOĆIĆ,* and *Jela M. BURAZER*

Department of Fluid Mechanics, Faculty of Mechanical Engineering,
University of Belgrade, Belgrade, Serbia

*This paper presents results of our own velocity field measurements in a straight pipe swirl flow. These studies were conducted using an originally designed hot wire probe. Due to the specially tailored shape of the probe, it was possible to get four measurement points in the viscous sublayer. The time-averaged velocity field and the statistical moments of the second and third order are calculated based on the measured velocity components. Mathematical and physical interpretations of statistical characteristics and structures of turbulent swirl flow in the time domain are presented. On the basis of these results, deeper insight into turbulent transport processes can be obtained, as well as useful conclusions necessary for turbulent swirl flows modeling.*

Key words: *turbulent swirl flow, hot wire probe, velocity field*

## Introduction

Turbulent swirling flows were investigated by numerous researchers in the past decades. The first experimental results were presented in [1-4]. These papers analyze the pressure and the mean velocity distributions, as well as the diameter of the vortex core (the so-called *dead water* region) [5].

The turbulent structure of swirling turbulent flows in long straight pipes was investigated for different combinations of parameters, such as various levels of swirl intensity, Reynolds numbers, pipe diameter, swirl generator, pipe roughness and the initial velocity profiles in [6-14].

A mathematical description of turbulent swirling flow in circular pipe is given in papers [15-22]. Calculations of turbulent shear stresses and turbulent viscosity based on the measured time averaged velocities and pressure from point to point in a single cross section of a pipe are given in [23-27].

The results of Reynolds stresses measurements in turbulent swirling flows in a pipe are presented in [28-35].

This paper discusses the results of the measurements obtained using a unique measurement calibration technique. An added value to the swirling flow family of data are the measurements obtained in the viscous sublayer achieved by the small size hot-wire specifically designed for this experiment.

---

\* Corresponding author, e-mail: mlecic@mas.bg.ac.rs

S692

Lečić, M. R., *et al.*: An Experimental Investigation and Statistical Analysis…
THERMAL SCIENCE, Year 2017, Vol. 21, Suppl. 3, pp. S691-S704

## Experimental equipment and methods

The experimental rig, the measuring and the calibration equipment are presented in great detail in [35, 36]. The layout of the experimental rig is shown in fig. 1. The main components are the pipe and the axial fan that is mounted at the pipe's inlet. The axial fan represents a swirl generator. The inner diameter of the pipe is $D = 398$ mm while the test section is located at the distance of $x/D = 17.5$ from the pipe's inlet.
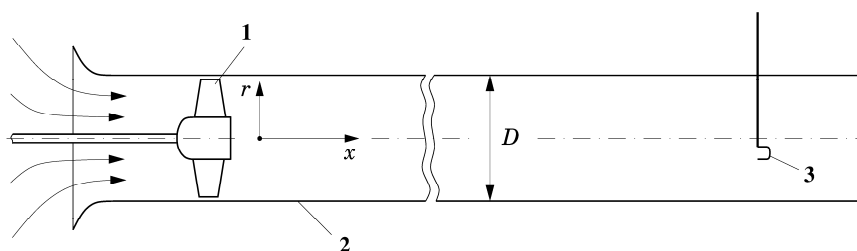


**Figure 1. Experimental rig: (1) Axial fan, (2) Circular pipe, (3) Hot-wire probe**

Internal statistically steady flow field in the cylindrical geometry of the pipe was in-vestigated, so the cylindrical coordinate system ( $x$ **,** $r$ **,** $\varphi$ ) is used and $\tilde{u}$**,** $\tilde{v}$ and $\tilde{w}$ are defined as instantaneous axial, radial and circumferential velocity components respectively. The coor-dinate system and velocity components are shown in fig. 2.

In order to measure all three components of instantaneous velocity, an in-house hot-wire probe was designed and built to measure all three velocity components of the instantaneous velocity. Previous research of turbulent swirling flow in pipes has shown that the radial velocity component is much smaller than the components in axial and circumferential directions, [26, 27, 31, 33, 37]. This finding provided a rationale for using a hot-wire probe with two sensors instead of three. In order to achieve higher measurement accuracy, a V-type probe is selected for the flow field under investigation as the velocity field is nearly homogeneous in the measuring volume of this probe type, [36]. On the other hand, the usage of an X-wire probe is not considered appropriate due to the significant mean velocity gradients in the radial direction of the flow (perpendicular to the pipe wall), [33].
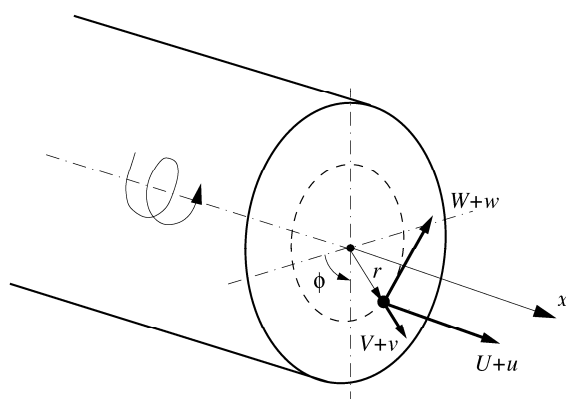


**Figure 2. Turbulent swirling flow in the pipe. Cylindrical coordinate system ( $x,r,\varphi$ ) and corresponding velocity components; $\tilde{u} = U + u$, $\tilde{v} = V + v$ and $\tilde{w} = W + w$**

The hot-wire probe used for measurements in this research, designated as VP-2vs, is unique. The sketch of the probe is shown in fig. 3. The probe sensors are made of Tungsten wire 2.5 μm in diameter and the length of 0.7 mm. The present V-wires probe is sufficiently

long in terms of the wire diameter ($l/d$ = 280) to minimize the end conduction effects resulting in an approximately uniform temperature distribution along the wire [33]. The sensors are welded to the tips of the tiny prongs made of stainless steel. The calibration procedure and conditions are described in details in [36].

The prongs are 0.4 mm in diameter, while they are tapered to 75 μm at the tip. The sensor prongs have the size and shape which enables measurements in vicinity of the pipe wall, *i. e.* in the viscous sublayer, [35, 36, 38].
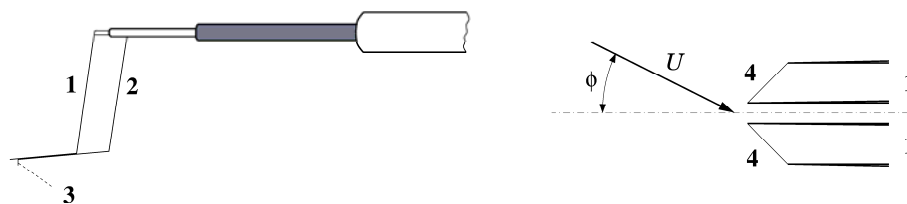


**Figure 3. Sketch of VP-2vs hot-wire probe used in experiments where (1) prongs of the sensor, (2) additional, fifth prong, (3) pin at the end of the fifth prong, (4) sensors**

The probe also has a fifth, slightly shorter prong. It is curved at the end, so it forms a kind of short pin. This pin is perpendicular to the plane of the sensor and is used for controlling the distance from the wall as it approaches it during measurements. When the probe approaches the pipe wall, the pin is the first part of the probes which makes contact with the wall. On the other hand, a piece of thin metal foil 0.03 mm in thickness is glued to the pipe wall. This metal foil and the fifth prong are connected to the DC circuit. When the pin touches the metal foil, the electrical circuit is closed and the LED diode turns on. At that moment, the sensors are located at a distance of 0.8 mm from the wall. In this way, the precise and repeat-able relative positioning between the probe and the pipe wall is secured.

Axisymmetry of the flow is determined by the series of previous measurements. The symmetry of the flow about the pipe axis is established for $x/D = 17.5$, hence all measurements were performed for the constant azimuth angle for the given location. The measuring points (total of 25) are specified in tab. 1 in a form of dimensionless coordinate $r/R$ and corresponding distance, $y$ [mm], from the wall. It should be noted that the four measuring points are located at a distance less than 1 mm from the pipe wall for a pipe $D = 398$ mm in diameter where the nearest measuring point from the wall is $y = 0.4$ mm. The smallest distance quoted in reference [33] was 2 mm from the pipe wall for a pipe $D = 150$ mm, which is greater distance in absolute and relative values in respect to these measurements.

While measurements are taken, the sensors of the VP-2vs probe are positioned in the tangential plane of the pipe. In addition, the radial component of velocity has to be very small in comparison to the other two components. As the probe approaches the pipe axis, the accuracy of the probe positioning becomes smaller. Also, in the area near the pipe axis the relative influence of the radial velocity, no matter how small it is, on voltage signals of the sensors is significant. Control measurements enabled us to choose a measuring point closest to the axis with appropriate measuring accuracy.

However, this probe showed significant advantages in measurements of turbulent swirl flow field near the pipe wall. It is well known that the wall region even for the simplest turbulent flows has a very complex structure. This complex structure is investigated in this

S694

Lečić, M. R., *et al.*: An Experimental Investigation and Statistical Analysis…
THERMAL SCIENCE, Year 2017, Vol. 21, Suppl. 3, pp. S691-S704

paper. Statistical characteristics in the wall region are very important for calculation of turbulent transfer and turbulence modeling.

**Table 1. Measuring points**

| Measuring point | 1 | 2 | 3 | 4 | 5 | 6 | 7 | 8 | 9 |
|---|---|---|---|---|---|---|---|---|---|
| $y/R$ | 0.15 | 0.20 | 0.25 | 0.30 | 0.35 | 0.40 | 0.45 | 0.50 | 0.55 |
| $y$ [mm] | 170 | 160 | 150 | 140 | 130 | 120 | 110 | 100 | 90 |
| **Measuring point** | **10** | **11** | **12** | **13** | **14** | **15** | **16** | **17** | **18** |
| $y/R$ | 0.60 | 0.65 | 0.70 | 0.75 | 0.80 | 0.85 | 0.90 | 0.95 | 0.0715 |
| $y$ [mm] | 80 | 70 | 60 | 50 | 40 | 30 | 21 | 10 | 5.7 |
| **Measuring point** | **19** | **20** | **21** | **22** | **23** | **24** | **25** | | |
| $y/R$ | 0.9865 | 0.9915 | 0.9925 | 0.996 | 0.997 | 0.9975 | 0.998 | | |
| $y$ [mm] | 2.7 | 1.7 | 1.5 | 0.8 | 0.6 | 0.5 | 0.4 | | |

Bulk velocity $U_m$ and Reynolds number in the experiment were:

$$U_m = \frac{4\dot{V}}{D^2\pi} = 3.06\,\text{m/s} \quad \text{and} \quad \text{Re} = \frac{U_m D}{\nu} = 8100 \tag{1}$$

while the swirl intensity $\theta$ and the swirl number $\Omega$ in the measuring section were:

$$\theta = \frac{\int_0^R rW^2U\,\text{d}r}{\int_0^R rU^3\,\text{d}r} = 1.87 \quad \text{and} \quad \Omega = \frac{2\int_0^R UWr^2\,\text{d}r}{R^3U_m^2} = 1.22 \tag{2}$$

where $R = D/2$ is the pipe radius. The hot wire calibration and measurement procedures are given in [36] in great detail. The basic analysis of measurement signal is based on the algorithm given in [39], which is implemented in C code. Further statistical analysis is presented in this paper.

It is also worth noting that changes of the integral and the local characteristics of turbulent swirling flows are much more evident in the radial than in the axial direction. Studies by many authors [28, 29, 31, 33, 35] pointed out the similarity of statistical parameters distributions of turbulence in different cross-sections of the pipe. Therefore, this comprehensive set of measurements in the characteristic measuring section $x/D = 17.5$, is a significant supplement to the database obtained by other authors.

## Statistical analysis of measured velocity field

During calibration and measurements, continuous voltage signals generated by the sensors $\tilde{e}_i(i = 1, 2)$ of the probe VP-2vs are recorded for a defined period of time $T_s$. The instantaneous voltage signal $\tilde{e}_i$ is converted by a two-channel analog-to-digital (A/D) converter to digital, discrete signals of $N$ samples $\tilde{e}_{Ni} = \tilde{e}_{Ni}[(n-1)\Delta t_s]$. The position of a sample in a sample array of digitized signals is denoted by $n \in \{1, …, N\}$, while $\Delta t_s\,[\text{s}]$ is the sample

Lečić, M. R., *et al.*: An Experimental Investigation and Statistical Analysis…
THERMAL SCIENCE, Year 2017, Vol. 21, Suppl. 3, pp. S691-S704

S695

interval. The data is saved to a computer hard drive for further statistical post analysis of the acquired data.

The selection of sample frequency $f_s = 1/\Delta t_s$ , or sample time step $\Delta t_s$ is based on the sampling Shannon-Nyquist theorem, [40]. According to the theorem, a continuous signal of limited range, with $f_m$ maximum frequency, can be fully reconstructed if the analog signal is digitized with the sampling frequency $f_s$, where $f_s > 2 f_m$. In this investigation the sampling frequency of $f_s = 20$ kHz was chosen, which is much larger than the minimal required frequency [35].

The first phase of statistical analysis of digital signals is completed after successful measurements with previously calibrated VP-2vs probe. In this phase, a 2-D array $(\tilde{u}_n, \tilde{w}_n)$ of length *N*, is obtained from the voltage samples. Quantities $\tilde{u}$ and $\tilde{w}$ are axial and circumferential components of instantaneous velocity acquired at a single measurement point, *i. e.* very small volume.

After the first phase is completed, a more detailed statistical analysis on the same data set of discrete random variables $\tilde{u}_n$ and $\tilde{w}_n$ is performed. At the beginning of the second phase, the mean velocities *U* and *W* are calculated as follows:

$$U = \frac{1}{N}\sum_{n=1}^{N}\tilde{u}_n \quad \text{and} \quad W = \frac{1}{N}\sum_{n=1}^{N}\tilde{w}_n \tag{3}$$

Further calculations are performed on velocity fluctuations, with the samples of velocity fluctuations being calculated as follows: $u_n = \tilde{u}_n - U$ and $w_n = \tilde{w}_n - W$.

The *k*-th empirical central moment $u^k$ is calculated using the formula:

$$\overline{u^k} = \frac{1}{N}\sum_{n=1}^{N}u_n^k \tag{4}$$

In the statistical theory of turbulence, besides central moments, mixed moments or correlation central moments are important for analyzing turbulent transport of momentum and turbulent energy. The $(k + s)^{th}$ empirical mixed moment of fluctuations *u* and *w* is calculated as follows:

$$\overline{u^k w^s} = \frac{1}{N}\sum_{n=1}^{N}u_n^k w_n^s \tag{5}$$

where $u_n$ and $w_n$ are the fluctuations of *u* and *w* in the same point in space. The mixed second moment $\overline{uw}$, also known as covariance $\text{cov}(u,w)$ represents one component of the Reynolds stress tensor. Correlation coefficient $R_{u^k w^s}$ is calculated as follows:

$$R_{u^k w^s} = \frac{\overline{u^k w^s}}{\sigma_u^k \sigma_w^s} \tag{6}$$

where $\sigma_u^k$ and $\sigma_w^s$ are the *k*-th central moment of fluctuation *u* and *s*-th central moment of fluctuation *w*, respectively.

## Experimental results and analysis

Measurement results of a velocity field in turbulent swirling flow with classical probes are shown in paper [37]. These results are limited only to profiles of mean velocities because classical probes are large relative to the characteristic length scales in the flow. The hot wire probe VP-2vs is very sensitive and is used for measurement of instantaneous velocity field. In this paper, besides profiles of axial and circumferential velocity components, profiles of central and mixed moments of second and third order are presented. These statistical quantities are very important in modeling of turbulent swirl flow field. An application within the Matlab software was developed to perform the data processing including the calculation of various statistical quantities.

### *Profiles of axial and circumferential velocities and turbulence intensity*

Measured radial profiles of the mean axial and mean circumferential velocities $U$ and $W$ are shown in figs. 4 and 5. The flow parameters are carefully chosen in order to obtain a velocity field that is characteristic for turbulent swirling flow. The presence of the recirculation flow area near the pipe axis is observed, while the profile of circumferential velocity has two maximums.

The flow field can be roughly divided into four areas, each of them having characteristic statistical properties and turbulence structures. In the vicinity of the pipe axis is the core area, where the mean circumferential velocity has the forced vortex distribution $W \propto r$. In the core area the recirculation flow can exist, but that is not the rule. In the core area the existence of recirculation flow was confirmed in many experimental investigations of turbulent swirling flows for certain conditions [6, 14, 26, 32, 33, 41]. For the flow parameter values defined by eqs. (1) and (2) in this study, the recirculation flow region was observed in the core area of the measurement section, and is clearly visible in fig. 4.
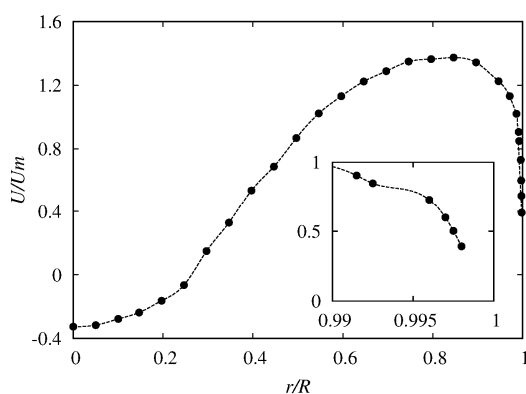


**Figure 4. Radial profile of mean axial velocity $U$; in the small diagram distribution of $U$ near the pipe wall is also given.**
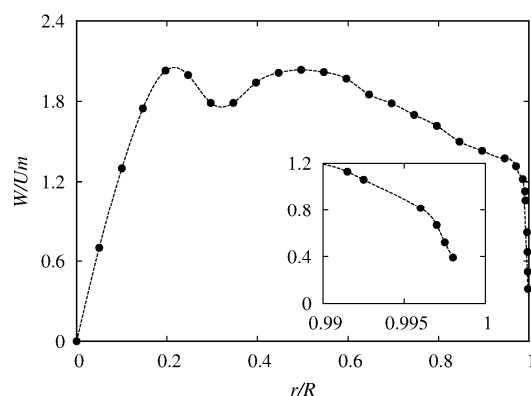
**Figure 5. Radial profile of mean circumferential velocity $W$; in the small diagram distribution of $W$ near the pipe wall is also given.**

Development and decay conditions of the recirculating region of swirling flows are still not sufficiently explained, especially not theoretically. However, it is clear that this phenomenon is directly related to the existence of the circumferential velocity and its profile and to the swirl intensity, defined by eq. (2), expressed by the parameter $\Omega$ or $\theta$. This relationship can be confirmed by analyzing Reynolds equation in the radial direction $r$,

assuming $\sigma_w^2 \ll W^2$. The validity of this assumption is substantiated by fig. 9. Taking this into account, the expression for the pressure distribution in the radial direction is expressed as follows:

$$P = P_w - \rho \int_r^R \left[ \frac{W^2}{r} - \frac{1}{r} \partial_r \left( r \overline{v^2} \right) \right] \mathrm{d}r \tag{7}$$

where $P_w$ represents the wall pressure. Based on the measurement results given in [26] eq. (7), and the Reynolds equation in the axial *x*-direction, it is obvious that the presence of circumferential velocity *W* has a great influence on the pressure distribution in the radial and the axial direction. The flow in the core area has the adverse streamwise pressure gradient ($\partial_x P > 0$) and when combined with the pressure distribution in the radial direction produces the inner recirculation in the flow field. In that process an additional radial transfer of axial momentum is also present.

In this 3-D problem, the pressure field condition is only one necessary condition for occurrence of the recirculation flow. The swirl intensity is another important parameter for recirculation to take place. In the experimental investigation of turbulent swirling flow in a pipe presented in this paper, the swirl intensity had the value of $\Omega = 1.22$. For this value, the recirculating flow is observed as shown in fig. 4. This is in good agreement with the results presented in [33], which shows that for $\Omega > 0.4$ the recirculation flow is present.

In the shear layer region, which connects the core region and the region of main flow, the circumferential velocity has a maximum value. Other investigations showed that all profiles of the circumferential velocity in the development of swirling flow in the pipe can be described by the theoretical model of the Rankine vortex, *i. e.* the model of forced-free vortex. Hence, the profile of circumferential velocity shown in fig. 5 can be described by the following equation:

$$W(r) = Cr^m \Leftrightarrow \frac{W}{U_m} = C_1 \left( \frac{r}{R} \right)^{-1} + f \left( \frac{r}{R} \right) \tag{8}$$

where the function takes the following form $f\left(r/R\right) = C_2\, r/R$ in case of a forced vortex. Parameters $C$, $C_1$, and *m* are functions of swirl intensity, or swirl number.

It is possible to determine experimental curves defined by the eq. (8) for various flow regions by the least square method applied to measured results of circumferential velocity. The eq. (8) predicts that circumferential velocity can be expressed as the sum of the potential vortex, $W \propto 1/r$ and the forced vortex, $W \propto r$. But, the radial profile of the circumferential velocity shown in fig. 5, with exceptions of the wall region, can be expressed in the first approximation as the sum of the two forced and the two free vortices. The constants of the first free vortex are $m \approx -1$ and $C = -0.5$ in the region $0.25 \le r/R \le 0.3$. The constants for the second free vortex, located in region $0.6 \le r/R \le 0.95$, are $m \approx -0.78$ and $C \approx 1.34$. This also implies the existence of three shear layers located between areas of the free and the forced vortices. Two shear layers are in the regions where the profile of the circumferential velocity has the local maximums, while the third one is in the region of its local minimum.

In the wall region, the high gradients of the mean axial and the mean circumferential velocity are present, which produce a very complex structure of turbulence. This region is very important in the processes of turbulent transfer of mass, momentum and energy. In this

paper, significant attention is dedicated to the investigations of statistical properties of the wall turbulence. The radial profiles of the mean axial and the mean circumferential velocity in the vicinity of the pipe wall are shown on the small diagrams in fig. 4 and fig. 5. It can be seen that in the region $1.5 \leq y[\text{mm}] \leq 0.8$ gradient $\partial_r W$ is larger than the gradient $\partial_r U$, while in the region $y < 0.4$ mm the two gradients have the same order of magnitude.

The turbulence intensity in the axial and the circumferential direction, $\sigma_u$ and $\sigma_w$, are calculated using the eq. (4) as follows:

$$\sigma_u = (\overline{u^2})^{1/2} \quad \text{and} \quad \sigma_w = (\overline{w^2})^{1/2} \tag{9}$$

The radial profile of the ratio $\sigma_u/\sigma_w$ is shown in fig. 6. Since the quantity $\sigma_u/\sigma_w$ shows the amplitude characteristics of the axial and the circumferential fluctuation velocity field, it is clearly seen from fig. 6 that the turbulence intensity $\sigma_w$ is greater than $\sigma_u$ in almost the entire cross-section, except in the domain $0.42 \leq r/R \leq 0.5$ and at the measured points $r/R = 0.3$ and $r/R = 0.998$. This is due to the relatively high swirl intensity and the higher values of the mean circumferential velocity $W$ in comparison to the values of the mean axial velocity in almost every measuring point in the cross-section, with exception in the immediate vicinity of the wall, as seen in fig. 6 and fig. 7.
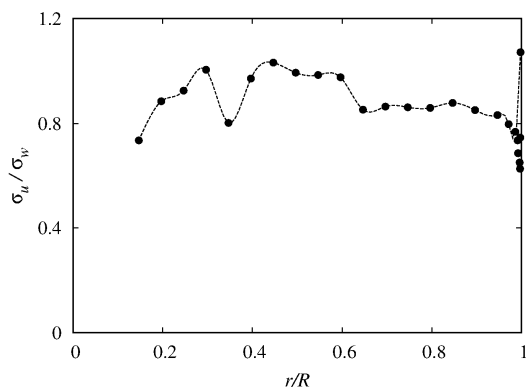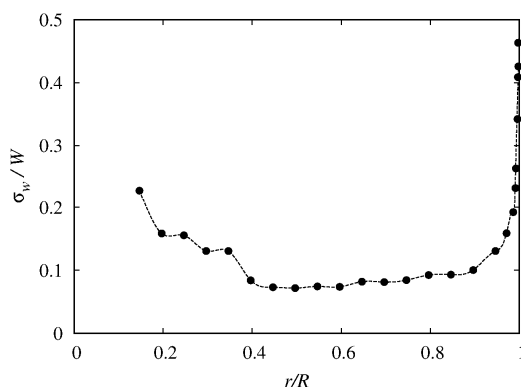


**Figure 6. Radial profile of the ratio $\sigma_u/\sigma_w$**

**Figure 7. Turbulence intensity in the circumferential direction**

The radial distribution of the ratio $\sigma_u/\sigma_w$ indicates the anisotropy of turbulence in the whole cross-section. More pronounced effects of anisotropy are observed in the core and the wall flow regions. The radial profile of normalized turbulence intensity $\sigma_w/W$ is shown in fig. 7. Values of the normalized turbulence intensity $\sigma_w/W$ attain a magnitude of about 20% in the flow core, about 15% in the shear layer, and between 8-10% in the region of the primary flow. Near the wall for $r/R > 0.9$, these values are increasing rapidly. In the wall proximity $1\text{mm} \leq y \leq 0.4$ mm, the values of $\sigma_w/W$ vary in the range 0.26 to 0.47. The ratio $\sigma_w/W$ attains the highest value of 0.47 in the vicinity of the wall as measured by the available probe at the closest distance $y = 0.4$ mm from the wall.

From the diagrams shown in figs. 4-7, it is clear that values of the ratio $\sigma_u/U$ and $\sigma_w/W$ have the same orders of magnitude. Based on the measurements, it can be concluded that a strong interaction between mean velocity field $U_i$ and fluctuation velocity

Lečić, M. R., *et al.*: An Experimental Investigation and Statistical Analysis…
THERMAL SCIENCE, Year 2017, Vol. 21, Suppl. 3, pp. S691-S704

S699

field $u_i$ occurs in this type of flow. This interaction is also clearly visible in the radial profiles of the mixed correlation moments of second ($Q_{ij}$) and third order ($Q_{ijk}$).

## Moments of second and third order and mixed moments of second and third order

Radial profiles of second order central moments $\overline{u^2} = \sigma_u^2$ and $\overline{w^2} = \sigma_w^2$ scaled with $U_m^2$ and with special attention to their changes in the wall region are shown in figs. 8 and 9. Quantities $\sigma_u^2$ and $\sigma_w^2$ reach their maximum values in the core region and in the shear layer region. They have smaller, nearly constant values in the region of primary flow. In the wall region (small diagrams in figs. 8 and 9), moments $\sigma_u^2$ and $\sigma_w^2$ again reach their peak values, proportional to normal turbulent stresses in axial and circumferential direction. This distribution of normal stresses is a consequence of the maximum values of circumferential velocity, significant changes of the velocity field in the radial direction, turbulence production and turbulent diffusion from regions of high gradients of axial and circumferential velocity.
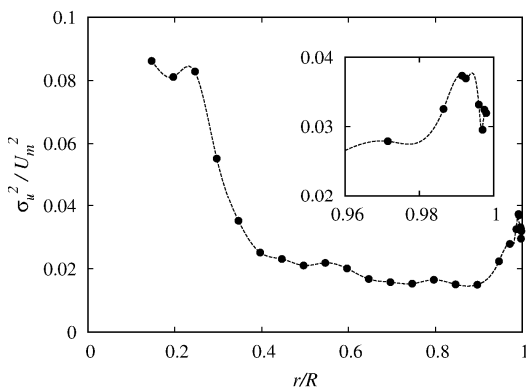


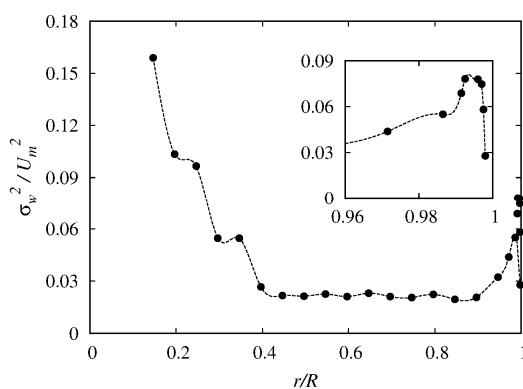**Figure 8. Radial profile of central moment of second order $\sigma_u^2$**

**Figure 9. Radial profile of central moment of second order $\sigma_w^2$**

In the region of primary flow, for values $0.4 \leq r/R \leq 0.9$, radial distributions of $\sigma_u$ and $\sigma_w$ are nearly uniform, with normalized values about 0.02 (figs. 9 and 10). In the region $0.9 \leq r/R \leq 0.9925$ normal turbulent stresses have very high gradients. In the vicinity of the wall, for $1.5 < y[\text{mm}] < 1.7$, the moment $\sigma_u^2$ reaches maximum value, but in comparison to its maximum values in the core and shear layer region, it is twice as small. Similar behavior is observed for the radial distribution of the central moment $\sigma_w^2$. Near the wall, it has a maximum value in the range $0.8 \leq y[\text{mm}] \leq 1.5$, and it is twice as small than its value in the core region, located at the point $r/R = 0.15$. In the region $y < 1.3$ mm, due to the no-slip condition at the wall, damping of fluctuation velocities is present, so the values of $\sigma_u$ and $\sigma_w$ are decreasing, from maximum value to the value of zero at the wall. This damping effect is more pronounced at the central moment $\sigma_w^2$, which can be seen on small diagrams in figs. 8 and 9. With the exception of the core and shear layer region, it can be concluded that in the wall region, for $0.8 < y[\text{mm}] < 1.7$ the moments $\sigma_u^2$ and $\sigma_w^2$, reach their maximum values. It should be emphasized that the values of the moment $\sigma_w^2$ are nearly twice as large as the values of the moment $\sigma_u^2$ in the core, shear layer and in the wall region. The reasons for that are very high swirl number and mechanisms of production of turbulence kinetic energy.

Statistical moments of second order $\sigma_u^2$ and $\sigma_w^2$, fluctuation intensities $\sigma_u$ and $\sigma_w$, and correlation moment of second order (or turbulent shear stress) $\overline{uw}$ provide data about amplitude and the correlation level of axial and circumferential velocities.

The radial profile of the correlation moment $Q_{uw} = \overline{uw}$ is shown in fig. 10. Values of moment $\overline{uw}$ are calculated using the formula given in eq. (5). Changes in the turbulent swirling flow field in both the axial and radial directions create additional mechanisms of turbulent transfer of momentum $Q_{uw}$. This transfer is directly related to the development of turbulent swirling flow, *i. e.* with transformation of the circumferential velocity profile in axial direction. It is clear from fig. 10 that turbulent or Reynolds shear stress $-\rho\overline{uw}$ has peak values in the same regions of cross-section like $\sigma_u$ and $\sigma_w$. Values of $\overline{uw}$ in the region of primary flow are very small, and are two to four times smaller than values of $\sigma_u^2$ and $\sigma_w^2$. Correlation moment $\overline{uw}$ changes its sign and reaches the highest positive value in the wall region. These values are significantly smaller than values of moments $\sigma_u^2$ and $\sigma_w^2$ in the same region. The radial profile of the correlation coefficient $R_{uw} = \overline{uw} / (\sigma_u \sigma_w)$ is shown in fig. 11. Normalized correlation moments are calculated using formula given in eq. (6).
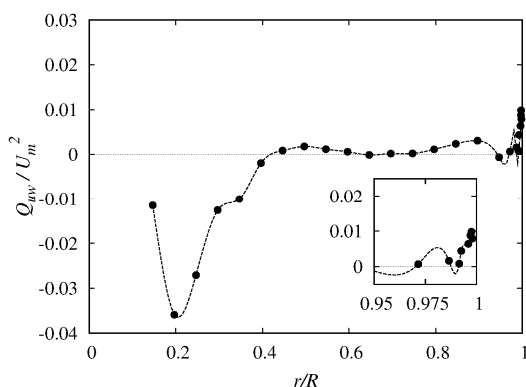


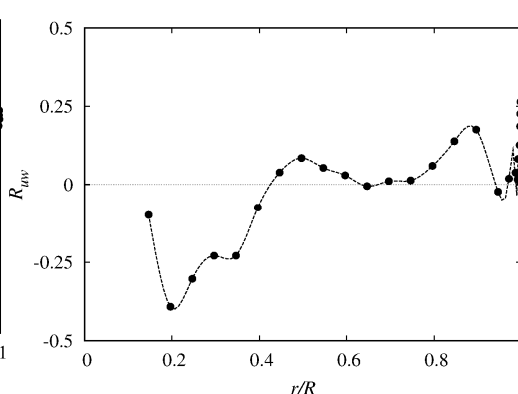**Figure 10. Radial profile of turbulent shear stress $\overline{uw}$**

**Figure 11. Radial profile of correlation coefficient $R_{uw}$**

The correlation coefficient $R_{uw}$, like the correlation moment $\overline{uw}$, changes its sign and has the highest negative values in the shear layer region, while in the wall region it has the highest positive values, or local maximum. Gradients of the mean axial $U$ and circumferential velocity $W$ in the axial direction have a big influence on the radial distribution of the correlation coefficient $R_{uw}$. This observation follows from analysis of the production terms $P_{\alpha\beta}$ in transport equations for turbulent stresses. These terms are as follows:

$$P_{uv} = -\overline{uv}\left(\partial_x U + \partial_r V\right) + \overline{uw}W / r - \sigma_v^2 \partial_r U - \sigma_u^2 \partial_x V \tag{10}$$

$$P_{uw} = -\overline{uw}\left(\partial_x U + V / r\right) - \overline{uv}\,\partial_r W - \overline{vw}\partial_r U - \sigma_u^2 \partial_x W \tag{11}$$

$$P_{vw} = -\overline{vw}\left(\partial_r V + V / r\right) - \overline{uv}\,\partial_x W - \overline{uw}\partial_x V - \sigma_v^2 \partial_r W + \sigma_w^2 W / r \tag{12}$$

From previous analyses and eqs. (10)-(12), it can be concluded that the existence of the swirl has a significant influence on the second order correlation moments. Measurements show that these moments have significant changes in the radial direction, and they reach their

maximum values in the shear layer and wall region. The anisotropy of turbulence and inhomogeneous distribution of statistical moments are also visible. This is mainly due to significant changes in the mean velocity field.

The diffusion terms $T_{\alpha\beta}^R = -\partial_k Q_{\alpha\beta k}$ in transport equations for Reynolds stresses have the correlation moments of the third order $Q_{\alpha\beta k}$. By the use of eq. (6) we can calculate the correlation coefficients $R_{mnp} = Q_{mnp}/\sigma_m \sigma_n \sigma_p$. Radial profiles of correlation coefficients of third order $R_{u^2 w}$ and $R_{uw^2}$ are shown in figs. 12 and 13.

The correlation coefficient $R_{u^2 w}$ changes its sign - it is negative in the core and wall regions, and positive elsewhere. It reaches the highest negative values in the vicinity of the wall, which is visible in fig. 12. This fact shows that convective transfer of turbulent kinetic energy is done by negative fluctuations of circumferential velocity. In other regions of cross-section, with the exception of the core region, this transfer is done by the positive fluctuations of circumferential velocity. A completely different situation occurs with the correlation coefficient $R_{uw^2}$. It has negative values across almost the entire cross-section, except near the wall where it changes sign and has positive values, fig. 11. From this radial distribution of $R_{uw^2}$, it can be concluded that the convective transfer of turbulent kinetic energy $\sigma_w^2$ by fluctuation of the axial velocity is mainly in the positive direction of the *x* axis, except in the wall region.
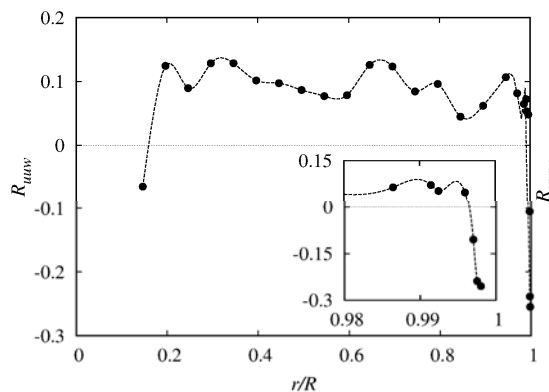
**Figure 12. Radial profile of third order correlation coefficient $R_{uuw}$**
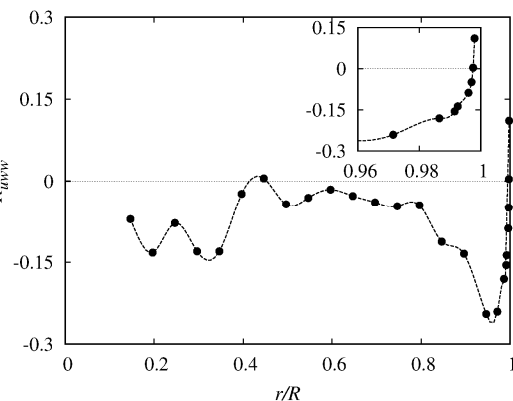
**Figure 13. Radial profile of third order correlation coefficient $R_{uww}$**

It should be emphasized that the distribution of correlation coefficients $R_{ijr}$ is very significant for processes of turbulent transfer and modeling of turbulent swirling flows. For deeper insight into the turbulence structure, additional measurements and analysis of statistical moments of higher order are needed.

**Conclusions**

In this paper measurements of the velocity field in turbulent swirling flow in a straight, circular pipe are presented and analyzed. Mathematical interpretation and physical explanation of statistical parameters and turbulence structure in swirling flows are given. With these results it is possible to get significant insight in processes of turbulent transfer and obtain usable conclusions for modeling of turbulent swirling flows.

**S702**

Lečić, M. R., *et al.*: An Experimental Investigation and Statistical Analysis…
THERMAL SCIENCE, Year 2017, Vol. 21, Suppl. 3, pp. S691-S704

Parameters of turbulent swirling flow investigated in this paper are carefully chosen, in order to get a characteristic flow field for this type of flow. In the region near the pipe axis (core region) recirculation flow exists, while the radial profile of circumferential velocity has two local maxima. Radial distributions of turbulence intensities in the axial and circumferential directions show a high level of anisotropy across the entire cross-section. A strong interaction between the mean and fluctuating velocity fields is also detected. The distribution of normal turbulent stresses is the result of turbulence production and turbulent diffusion from regions of high gradients of axial and circumferential velocity. The same behavior is observed in the distribution of turbulent shear stress.

Anisotropy of turbulence is also confirmed in the inhomogeneous distribution of third order mixed moments, which are related to the observed significant changes in the mean velocity field. Also, the convective transfer of kinetic energy of turbulence by fluctuation of the axial velocity in the circumferential direction is mainly in the positive direction of the $x$-axis. It is important to mention that four measuring points are at a distance less than 1 mm from the pipe wall. Thus, it can be said that unique results of measurements in a viscous layer are shown in this paper.

## Acknowledgment

## Nomenclature

$Q_{uw}$ – correlation moment of the second order, [-]
$R_{uw}$ – correlation coefficient of the second order, [-]
$U_m$ – bulk velocity, [ms$^{-1}$]
$U, W$ – mean velocity in axial ($x$) and circumferential ($\varphi$) directions, [m/s]
$u, w$ – fluctuating velocities in axial ($x$) and circumferential ($\varphi$) directions, [ms$^{-1}$]
$\dot{V}$ – volume flow rate, [m$^3$s$^{-1}$]

*Greek symbols*

$\theta$ – swirl flow intensity, [-]
$\sigma_u$ – turbulence intensity in the axial direction, [ms$^{-1}$]
$\sigma_w$ – turbulence intensity in the circumferential direction, [ms$^{-1}$]
$\sigma_u^2$ – central moment of the second order, [m$^2$s$^{-2}$]
$\sigma_w^2$ – central moment of the second order, [m$^2$s$^{-2}$]
$\Omega$ – swirl number, [-]

## References

[1]   Meldau, E., Swirl Flow in Axisymmetrical Spaces (in German), Ph. D. thesis, Tech. University Hannover, Hanover, Germany, 1935
[2]   Schiebeler, W., Air Swirl Flow in Pipe Behind Radial Guide Vanes (in German), Mitteilungen aus dem Max-Planck-Institut fr Strmungsforschung, (1955), 12, Gottingen, Germany
[3]   Schlünkes F., Measurements in Air Flow with Constant Swirl in a Straight Circular Tube (in German), Voith Forsch. u. Konstr.5, (1959), pp. 2.1-2.11
[4]   Laux, H., Contribution to the Experimental Investigation of Swirl Flow in Circular Tubes (in German), Ph. D. thesis, Technical University, Berlin, 1961
[5]   Gupta, A. K., *et al.*, *Swirl Flows*, Abacus Press, Preston, UK, 1984.
[6]   Baker, D. W., Sayre, C. L., Decay of Swirling Flow of Incompressible Fluids in Long Pipes, *Proceedings*, 1st Symposium on Flow, Its Measurement and Control in Science and Industry, Pittsburgh, Penn., USA, Vol. 1, Part 1, 1971,  pp. 301-312

[7]  Lea, J.F., Price, D. C., Mean Velocity Measurements in Swirling Flow in a Pipe, *Proceedings*, 1st Symposium on Flow, Its Measurement and Control in Science and Industry, Pittsburgh, Pen., USA, Vol. 1, Part 1, 1971,  pp. 313-317

[8]  Senoo, Y., Nagata, T., Swirl Flow in Long Pipes with Different Roughness, *Bull. JSME, 15* (1972), 90, pp. 1514-1521

[9]  Sawatzki, O., Swirl flow in Long Circular Pipes (in German), Strömungsmechanik und Strömungsmaschinen, (1972), 12, pp. 1-33

[10]  Ito, S., *et al.*, Decay process of swirling flow in a circular pipe, *Int. Chem. Eng.*, *19* (1979), 4, pp. 600-605

[11]  Nejad, A. S., Ahmed, S. A., Flow Field Characteristics of an Axisymmetric Sudden Expansion Pipe Flow With Different Initial Swirl Distribution, *Int. Heat and Fluid Flow*, *13* (1992), 4, pp. 314-321

[12]  Khezzar, L. Velocity Measurements in the Near Field of a Radial Swirler, *Experimental Thermal and Fluid Science*, *16*, (1998), pp. 230-236

[13]  Yajnik, K. S., Subbiah, M. V., Experiments on Swirling Turbulent Flows, Part 1, Similarity in Swirling Flows, *J. Fluid Mech.*, *60* (1973), Part 4, pp. 665-687

[14]  Escudier, M. P., Keller, J., Recirculation in Swirling Flow: A Manifestation of Vortex Breakdown, *AIAA Journal*, *23* (1985), 1, pp. 111-116

[15]  Gollatz, L., Görtler, H., Weak Swirl Flow in Pipes (in German), *ZAMP, 5* (1954), pp. 95-110

[16]  Einstein, H. S., Li, H., Steady Vortex Flow in a Real Fluid, *Proceedings,* Heat Transfer & Fluid Mechanics, Institute Palo Alto, Cal., USA, 1951, Vol. 4, pp. 33-42

[17]  Kreith, F., Sonju, O. K., The Decay of a Turbulent Swirl in a Pipe, *J. Fluid Mech.*, *22* (1965), Part 2, pp. 257-271

[18]  Rochino, A., Lavan, Z., Analytical Investigations of Incompressible Turbulent Swirling flow in Stationary Ducts, *J. Appl. Mech.*, *36* (1969), 2, Series E, pp. 151-158

[19]  Akiyma, T., Ikeda, M., Fundamental Study of the Fluid Mechanics of Swirling Pipe Flow with Air Suction, *Ind. Eng. Chem. Process Des. Dev.*, *25* (1986), pp. 907- 913

[20]  Yoshizawa, A., *et al.*, Variational Approach to Turbulent Swirling Pipe Flow with the Aid of Helicity, *Phys. Fluids*, *13* (2001), 8, pp. 2309-2319

[21]  Strscheletzky, M., Separation Layers (in German), Fortschritt-Berichte der VDI-Zeitschriften Reihe 7, No. 32,  Dusseldorf: VDI-Verlag, Germany, 1972

[22]  Reader-Harris, M. J., The Decay of Swirl in the Pipe, *Int. Heat and Fluid Flow*, *15* (1994), 3, pp. 212-217

[23]  Scott, C. J., Rask, D. R., Turbulent Viscosities for Swirling Flow in a Stationary Annulus, *J. Fluids Eng., 95* (1973), 4, pp. 557-566

[24]  Murakami, M., *et al.*, An Experimental Study of Swirling Flow in Pipes, *Bull. JSME, 19* (1976), 128, pp. 118-126

[25]  Scott, C. J., Bartelt, K. W., Decaying Annular Swirl Flow with Inlet Solid Body Rotation, *J. Fluid Eng.*, *98* (1976), 1, pp. 33-39

[26]  Benišek, M. H., Investigation of the Swirling Flow in Long Lined Circular Pipes (in Serbian), Ph. D. thesis, Faculty of Mechanical Engineering, University of Belgrade, Belgrade, Serbia, 1979

[27]  Algifri, A. H., Bhardway, R. K., Rao Y. V. N., Prediction of the Decay Process in Turbulent Swirl Flow, *Proc. Inst. Mech. Engrs*, *201* (1987), 4, pp. 279-283

[28]  Weske, J. R., Sturov, G. E., Experimental Investigation of Turbulent Swirling Flow in a Cylindrical Tube, *Proc. Siberation Siv. Acad. Sci. USSR, 13* (1972), 3, pp. 3-7

[29]  Acrivellis, M., Investigations of Turbulent Swirl Flow Behind a Radial Guide Vanes (in German), Ph. D. thesis, Technical University Karlsruhe, Karlsruhe, Germany, 1973

[30]  Saito, S., *et al.*, Decay of Swirl in a Straight Pipe Flow, *Rep. Inst. High Speed Mech.*, *28* (1973), 260, pp. 43-76

[31]  Čantrak, S. M., Experimental Investigations of Statistical Properties of Swirling Flows in Pipes and Diffusers (in German), Ph. D. thesis, Technical University Karlsruhe, Karlsruhe, Germany, 1981

[32]  Kind, R. J., *et al.*, The Law of the Wall for Swirling Flow in Annular Ducts, *J. Fluids Eng.*, *111* (1989), 2, pp. 160-164

[33]  Kitoh, O., Experimental Study of Turbulent Swirling Flow in a Straight Pipe, *J. Fluid Mech.*, *225* (1991), pp. 445-479

[34]  Anwer, M., So, R. M. C., Swirling Turbulent Flow Through a Curved Pipe, *Experiments in Fluids*, *14* (1993), Dec., pp. 85-96

[35] Lečić, M. R., Theoretical and Experimental Investigation of Turbulent Swirling Flows (in Serbian), Ph. D. thesis, Faculty of Mechanical Engineering, University of Belgrade, Belgrade, Serbia, 2003

[36] Lečić, M. R. *et al*., Original Measuring and Calibration Equipment for Investigation of Turbulent Swirling Flow in Circular Pipe, *Experimental techniques, 38* (2014), 3, pp. 54-62

[37] Benišek, M. H. *et al*., Application of New Classic Probes in Swirl Fluid Flow Measurements, *Experimental Techniques, 34* (2010), 3, pp. 74-81

[38] Vukoslavčević, P., Petrović, D. *Multiple Hot-Wire Probes. Measurement of Velocity and Vorticity Vector Fields*, Montenegrin Academy of Sciences and Arts, Podgorica, 2000

[39] Lečić, M. *et al*., V-type Hot Wire Probe Calibration, *FME Transactions, 35* (2007), 2, pp. 55-62

[40] Proakis, J., Manolakis, D., *Digital Signal Processing: Principles, Algorithms, and Applications*, Macmillan Publishing Company, New York, USA, 1992

[41] Benišek, M. *et al*., Theoretical and Experimental Investigation of the Turbulent Swirling Flow Characteristics in Circular Pipes, *ZAMM, 68* (1988), 5, T 280-282